Available online at www.sciencedirect.com

ScienceDirect

journal homepage: www.jfda-online.com

Original Article

General survey of Fructus Psoraleae from the different origins and chemical identification of the roasted from raw Fructus Psoraleae

Junjun Yang [a,b], *Jing Yang* [a,b], *Jie Du* [a,b], *Yuxin Feng* [a,b], *Xin Chai* [a,b], *Mingming Xiao* [a,b], *Yuefei Wang* [a,b,*], *Xiumei Gao* [a,b,**]

[a] *Tianjin State Key Laboratory of Modern Chinese Medicine, Tianjin University of Traditional Chinese Medicine, Tianjin 300193, China*

[b] *Research and Development Center of TCM, Tianjin International Joint Academy of Biotechnology and Medicine, Tianjin 300457, China*

ARTICLE INFO

Article history:
Received 19 June 2017
Received in revised form
16 October 2017
Accepted 22 October 2017
Available online 1 December 2017

Keywords:
Fructus Psoraleae
β-glucosidase
Psoralenoside
Isopsoralenoside

ABSTRACT

Fructus Psoraleae, a traditional Chinese medicine, is widely used for preventing and treating various diseases such as vitiligo, osteoporosis and psoriasis. Coumarin, such as psoralenoside, isopsoralenoside, psoralen and isopsoralen, are important compounds in Fructus Psoraleae. In our study, ultra performance liquid chromatography coupled with diode array detector was employed for an excellent method validation for simultaneous quantification of psoralenoside, isopsoralenoside, psoralen and isopsoralen, which was further applied in performing general survey of Fructus Psoraleae from the different origins and chemical identification of the roasted from raw Fructus Psoraleae in the light of illuminating the transformed rule of psoralenoside and isopsoralenoside. There is a reciprocal relationship between (iso)psoralenoside and (iso)psoralen, and the total content remains balance in Fructus Psoraleae from the different origins. In addition, we found that (iso)psoralenoside in the powder of the raw Fructus Psoraleae could be easily transformed into (iso)psoralen in methanol aqueous solution, especially above 50% water, rather than the roasted one. Thus, we proposed a hypothesis that transformation between (iso)psoralenoside and (iso)psoralen was hindered by inactivation of β-glucosidase in the process of roasting Fructus Psoraleae, which was further verified by observing transformation of (iso)psoralenoside under the different conditions, such as temperature, pH and β-glucosidase. Therefore, we developed a feasible method to distinguish the roasted from raw Fructus Psoraleae by observing conversion from (iso)psoralenoside to (iso)psoralen in 50% methanol aqueous solution. In summary, these results pave the way for elevating quality standard for Fructus Psoraleae and distinguishing the salt-processed from raw Fructus Psoraleae.

* *Corresponding author*. Tianjin State Key Laboratory of Modern Chinese Medicine, Tianjin University of Traditional Chinese Medicine, No. 312 An Shan Xi Road, Nankai District, Tianjin 300193, China.

** *Corresponding author*. Tianjin State Key Laboratory of Modern Chinese Medicine, Tianjin University of Traditional Chinese Medicine, No. 312 An Shan Xi Road, Nankai District, Tianjin 300193, China.

E-mail addresses: wangyuefei_2006@hotmail.com (Y. Wang), gaoxiumei@tjutcm.edu.cn (X. Gao).

https://doi.org/10.1016/j.jfda.2017.10.009

1. Introduction

Known as Buguzhi in China, Fructus Psoraleae (FP), the dried and ripe fruit of *Psoralea corylifolia* L., which belongs to the family Leguminous, is widely used in Asian country as a traditional medicine. It has been employed for warming kidney and activating yang, promoting inspiration and checking diarrhea, according to Chinese pharmacopoeia (ChP) [1]. And lots of its active components, including monoterpene phenols, coumarins and flavonoids, have been demonstrated to have unique effectiveness against coronary artery disease [2], osteoporosis [3], bacterial infection [4] and vitiligo [5]. As chemical markers for quality control of FP [1], psoralen (P) and isopsoralen (IP) show various biological activities, such as antibacterial, anti-inflammatory [6,7], antitumor [8,9], estrogen-like effect [10,11] and antioxidant activities [12], and so forth.

With the continuously expanded clinical application of FP, toxicity problems, especially the liver toxicity, have been concerned by researchers and doctors. Cheung et al. [13] claimed that FP was recognized as one of the emerging hepatotoxins, in that P and its related chemicals may be responsible for the hepatotoxicity. Kong et al. [14] demonstrated that rats given P and IP (40 mg/kg) showed modest liver injury. P and IP affected hepatic microsomal cytochrome P450 and renal organic ion transport system. Our previous study [15] suggested that a significant increase of AUC and delayed elimination of P and IP were found through conversion of psoralenoside (PO) and isopsoralenoside (IPO) to P and IP by intestinal flora, which possibly worsened the liver toxicity. And according to ChP, only P and IP were the index components in FP. But, in the light of conversion between (I)PO and (I)P, we suggested that PO and IPO should be used as important quality markers for FP, together with the frequently used P and IP.

The ingredients of herbal medicines would be affected significantly by environment, collecting time, storage condition and processing [16,17], as well as FP, which may affect efficacy or even cause toxicity. Therefore, general survey of FP from the different origins should be performed, including the raw and salt-processed one. Furthermore, according to the market surveys, it is challenging to differentiate the raw and salt-processed FP, which have the different functions. Extrinsic feature of ninety-six batches FP was shown in Fig. S1 of supporting information, which resemble each other. So far, the salt-processed FP was only identified by morphological identification, microscopic identification [1,18], leading to erroneous judgment. In clinic, the salt-processed FP is used commonly. Therefore, establishment of a more reliable and simple method to identify the salt-processed FP is imperative.

Up to date, several methods including high performance liquid chromatography (HPLC) [19–21], ultra performance liquid chromatography (UPLC) [22], and high performance liquid chromatography–mass spectrometry (HPLC–MS) [23], were employed to determine the quantity of constituents in FP. But, some of the methods mentioned above suffered from limited compounds in FP except for PO and IPO [20,23] and longer analytical time [19–21]. Therefore, it is necessary to establish a simple and effective method to simultaneously determine the contents of PO, IPO, P and IP, and distinguish the salt-processed from raw FP.

In our study, a UPLC method was developed for the quantification of PO, IPO, P and IP in FP, which was applied to perform the general survey of ninety-six batches FP from the different origins and chemical identification of the salt-processed from raw FP in view of lighting transformed rule of PO and IPO. The aim of this paper was to provide experimental basis for improving quality standard for FP, and distinguish the salt-processed from raw FP, guaranteeing the safety and efficacy of clinic application of FP.

2. Materials and methods

2.1. Reagents and materials

The methanol was HPLC grade (Sigma Aldrich, St Louis, MO, USA). Formic acid was obtained from Meridian Medical Technologies (Columbia, MD, USA). Water used in the experiment was purified by a Milli-Q water purification system (Millipore, Billerica, USA). β-glucosidase was purchased from Sigma–Aldrich (St Louis, MO, USA). Phosphoric acid, disodium hydrogen phosphate, potassium dihydrogen phosphate and dipotassium hydrogen phosphate were bought from DAMAO Chemical Reagent Factory (Tianjin, China). Reference compounds (P and IP) were purchased from National Institute for Food and Drug Control (Beijing, China). PO and IPO with purity above 98% were identified by NMR, LC/MS, IR and UV in our lab.

Ninety-six batches FP, numbered as B-1 to B-96 (the raw and salt-processed FP) were purchased from the different markets of medicinal materials and identified by Professor Tianxiang Li, which were deposited in Tianjin State Key Laboratory of Modern Chinese Medicine. Sample information was summarized in Table S1 of supporting information.

The raw FP (B-5, B-51 and B-96) soaked with 4% salt solution at the ratio of 500 g:250 mL (*m*:*v*), according to ChP of 2015 edition, were divided into two parts separately. One moiety was dried under the shade at room temperature for 2 days and numbered as SK-5, SK-51 and SK-96, and others were processed by stir-frying at 150 °C for 10 min and numbered SP-5, SP-51 and SP-96, respectively.

2.2. Preparation of standard solutions

Four reference compounds were accurately weighted and directly dissolved in methanol to obtain stock solution, separately. Then, the combined standard solution containing 4 standards were prepared for constructing calibration curves. The standard solution was stored at 4 °C for further analysis.

Working standard solutions for calibration curves were obtained by diluting the combined standard solution with 30% methanol (*v*:*v*, 1:1) to obtain a series of different concentrations of these analytes, whose concentration ranges were 1.20–38.30 μg/mL for PO, 1.29–41.20 μg/mL for IPO, 3.17–101.40 μg/mL for P and 3.13–100.20 μg/mL for IP. All solutions were stored at 4 °C until analysis.

2.3. Sample preparation

For general survey of FP, every accurately weighed powder (0.5 g) was transferred into 100 mL volumetric flask. Methanol was added and sonicated for 30 min at 60 °C, then cooled to room temperature. Methanol was added to reach the scale of 100 mL and mixed. The solution was centrifuged at 14,000 rpm for 10 min. The supernatant was diluted with 30% methanol (v:v, 1:1) to obtain the sample solution.

For identifying the salt-processed from raw FP, the powder of samples was deposited in 100 mL volumetric flask. 50% methanol aqueous solution was added and sonicated for 30 min at 60 °C, then cooled to room temperature. 50% methanol aqueous solution was added to reach the scale of 100 mL and mixed. The solution was centrifuged at 14,000 rpm for 10 min. The supernatant was diluted with 30% methanol (v:v, 1:1) and injected immediately into UPLC system for analysis.

For studying transformation between (I)PO and (I)P in water under the different conditions, the testing solution of PO and IPO was prepared at a final concentration of about 50 μg/mL which was subjected to the different impact factors, such as temperatures (30 °C, 50 °C and 70 °C for 12 h), pH (2.0, 4.0, 6.0 and 8.0 for 12 h) and β-glucosidase (37 °C, pH at 5.0 for 19 h in 100 mM sodium acetate buffer). The aliquot of 2 μL solution per hour was directly injected into UPLC system for analysis.

2.4. UPLC analysis

Analysis was performed on a Waters ACQUITY UPLC system. The system was controlled by Empower Pro software (Waters). Gradient elution was performed on an ACQUITY UPLC BEH C18 column (2.1 × 50 mm, 1.7 μm) at 60 °C. The mobile phase was composed of 0.1% formic acid aqueous solution (A) and methanol (B). The gradient program applied was as follows: 0–6 min, 10–60% B. The wavelength employed was 246 nm. The flow rate was 0.3 mL/min and injection volume was 2 μL.

2.5. Method validation

The analytic method established in this study was validated for linearity, LOD, LOQ, precision (intra- and inter-day), repeatability, stability and recovery. Calibration curves were constructed based on the peak area of analytes (y) versus the corresponding concentrations (x) at six different concentrations in triplicate. The LOD and LOQ were determined by S/N at about 3 and 10 using standard solutions, respectively. The intra- and inter-day precisions were conducted with six replicate injections of the same sample solution performed on the same day and three consecutive days, respectively. To confirm the repeatability, six sample of the same origin were processed and analyzed. The stability of the sample solution stored in UPLC autosampler at 10 °C was investigated by replicate injection of the sample solution at 0, 1, 2, 4, 6, 8, 10 and 12 h. A recovery test was used to further evaluate the accuracy of method. Accurate amount of the mixed standard solution was added to 0.25 g sample powder, whose sample solution was further prepared and analyzed with the method described above.

2.6. Data processing

Contents of PO, IPO, P and IP obtained by utilizing different methods of extraction were displayed by GraphPad Prism 5.01 software (Graphpad software Inc., USA). The 'Spider-web' was made by Excel 2016.Lnk software.

3. Results and discussion

3.1. Optimization of extraction conditions

To obtain the optimal condition of sample preparation, many factors, including methods of extraction (soxhlet extraction recorded in ChP, refluxing extraction, ultrasonic extraction and ultrasonic extraction at 60 °C), the extraction solvents (0, 25, 50, 75 and 100% methanol in aqueous solution), the extraction time (20, 30 and 40 min), and the material/solvent ratio (1:100, 1:200 and 1:400 g/mL), were optimized by using univariate analysis. The results were shown in Fig. 1.

An interesting phenomenon has happened, when the raw and roasted FP were treated by different extraction solvents (0, 25, 50, 75 and 100% methanol in aqueous solution) using the four different methods of extraction described above except for soxhlet extraction. Noticeably, for the raw FP, compared with the contents of PO, IPO, P and IP obtained by soxhlet extraction, the formal method regulated by ChP, the quantitative results of selected compounds obtained by methanol extraction of the other three methods were consistent with that of soxhlet extraction. But, as methanol in aqueous solution decreased, the content of PO and IPO in the raw FP declined obviously, and P and IP increased remarkably, especially when methanol was below 50% in extraction solvent. Therefore we speculated that the conversion between (I)PO and (I)P was performed by β-glucosidase naturally present in plant [24,25], which was proved by releasing the powder of the raw FP to the boiled 50% methanol to prevent the conversion. In order to further verify this idea, the roasted grain of FP was prepared by keeping the raw FP at 150 °C for 2.5 h in oven. For the roasted FP, the outcomes obtained by methanol extraction using the three methods accorded with that by soxhlet extraction, except for ultrasonic extraction with lower extraction of PO and IPO. Along with the reduction of methanol in aqueous extraction solvent, the conversion between (I)PO and (I)P was not observed. Only the content of P and IP decreased slightly because of the lipophilic property.

Given that high extraction rate and efficiency, the 'Spider-web' mode [26,27] was employed to choose the best method by taking six characteristics into account, including the extraction efficiency of PO, IPO, P and IP, the extraction time, and the dealing time before extraction. The contents of PO, IPO, P and IP in the raw and roasted FP originated from different methods were marked as $C_{k\text{-}m}$ and C'_{k-m}, and the extraction time was labeled as t_k and t'_k, and dealing time before extraction was assigned as s_k and s'_k, respectively. The highest content of PO, IPO, P and IP derived from the tested method was marked as $C_{k\text{-}m}$ (max) and C'_{k-m} (max) in the raw or the roasted FP, respectively. The highest value of $1/t_k$ and $1/t'_k$ was respectively tagged as $1/t_k$ (max) and $1/t'_k$ (max), which was also applied for the

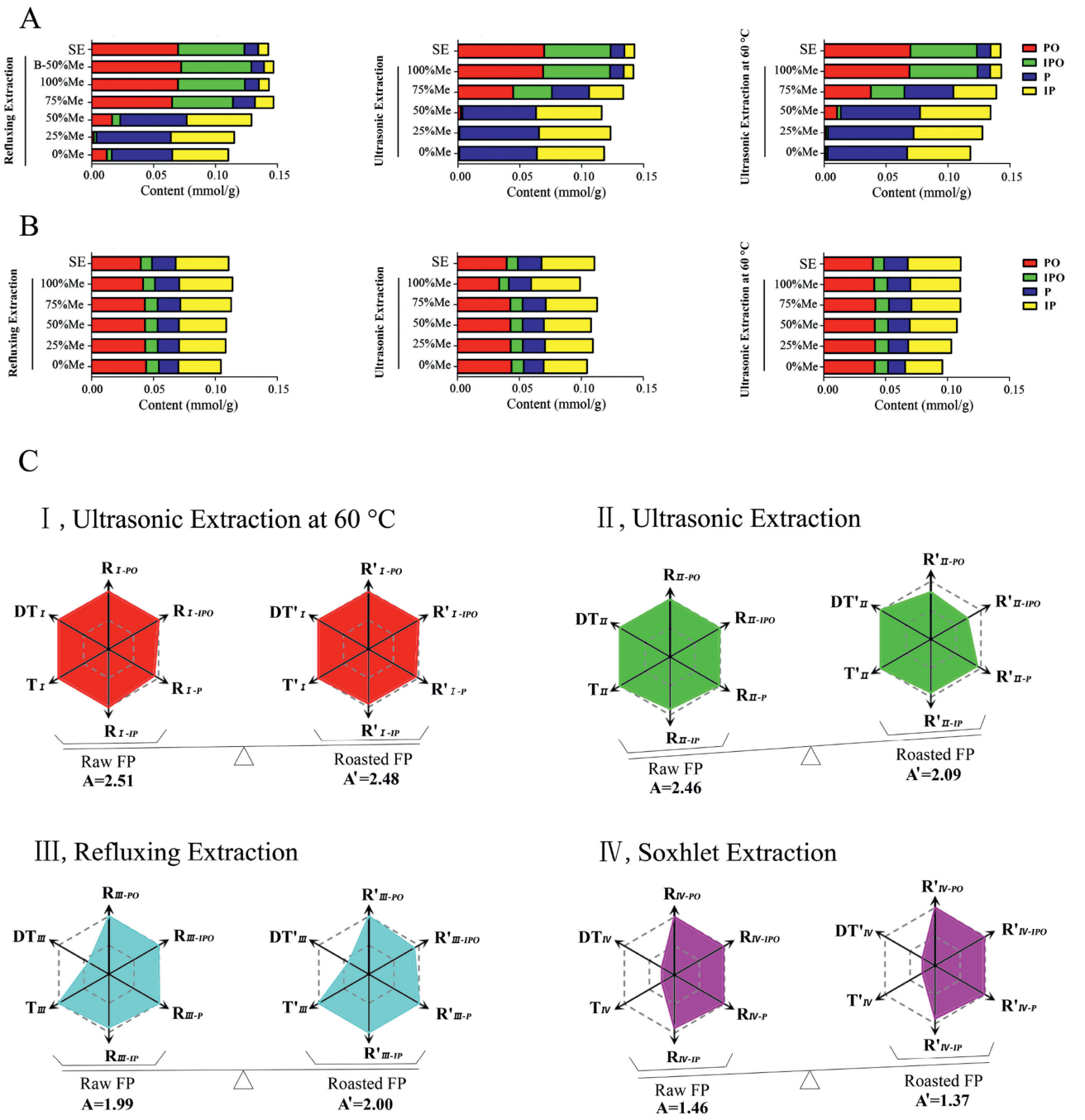

Fig. 1 – The histograms of PO, IPO, P and IP, and 'Spider-webs' obtained by the different methods employed for extracting the raw and roasted FP (SE, the soxhlet extraction method released by Chinese pharmacopoeia; B-50%Me, the boiled 50% methanol aqueous solution; A, the histograms of PO, IPO, P and IP in the raw FP extracted by different methods; B, the histograms of PO, IPO, P and IP in the roasted FP extracted by different methods; C, the 'Spider-webs' obtained by the different methods employed for extracting the raw and roasted FP).

dealing time before extraction (DT). The contents of PO, IPO, P and IP divided by their corresponding maximum, which was badged as $R_{k\text{-}m}$ and R'_{k-m} in the raw and roasted FP, and the inverse of dealing time and preparation time divided by their corresponding maximum, which was tagged as T_k and T'_k, and DT_k and DT'_k, separately.

Calculation formulae were as follows. *k* represented the methods of ultrasonic extraction at 60 °C (I), ultrasonic extraction (II), refluxing extraction (III) and soxhlet extraction recorded in ChP (IV); *m* represented the compounds of PO, IPO, P and IP.

$$R_{k-m} = C_{k-m}/C_{k-m}(\max) \quad R'_{k-m} = C'_{k-m}/C'_{k-m}(\max)$$

$$T_k = \frac{1}{t_k}\Big/\frac{1}{t_k}(\max) \quad T'_k = \frac{1}{t'_k}\Big/\frac{1}{t'_k}(\max)$$

$$DT_k = \frac{1}{s_k} \Big/ \frac{1}{s_k}(\max) \quad DT'_k = \frac{1}{s'_k} \Big/ \frac{1}{s'_k}(\max)$$

Take the method of ultrasonic extraction at 60 °C (I) as example, $R_{I\text{-}PO}$, $R_{I\text{-}IPO}$, $R_{I\text{-}P}$, $R_{I\text{-}IP}$, T_I, and DT_I were employed to build six dimensions of the 'Spider-web' (p_i) for the raw FP, and R'_{I-PO}, R'_{I-IPO}, R'_{I-P}, R'_{I-IP}, T'_I and DT'_I were used to establish six dimensions of the 'Spider-web' (p'_i) for the roasted FP. The 'Spider-webs' of the four methods were shown in Fig. 1. The shaded areas of the 'Spider-webs' were established to analyze and determine the most appropriate method, calculating formulae of which were employed for the raw (A) and roasted FP (A′) were as follows. The angle between two dimensions was marked as α and α', respectively.

$$A = \frac{1}{2} \times \sin\alpha \left(\sum_{i=1}^{n-1} p_i \times p_{i+1} + p_n \times p_1 \right)$$

$$A' = \frac{1}{2} \times \sin\alpha' \left(\sum_{i=1}^{n-1} p'_i \times p'_{i+1} + p'_n \times p'_1 \right)$$

In general, the extraction method, ultrasonic extraction at 60 °C, did not discriminate against the raw or roasted FP, which showed the balanced shaded area of the 'Spider-web' (A, 2.51 and A′, 2.48). Moreover, the highest value of the shaded area demonstrated the perfect extraction rate and efficiency compared with the other methods.

3.2. *Transformation of psoralenoside and isopsoralenoside under different conditions*

As mentioned above, PO and IPO can be transformed into P and IP in the raw FP rather than roasted FP, which suggested that transformation between (I)PO and (I)P may be influenced by the impacts of temperature, pH or β-glucosidase. Therefore, we have systematically performed the effect of temperature, pH, and β-glucosidase on conversion of PO and IPO (Fig. 2). As shown in Fig. 2, the remaining concentration of PO and IPO showed the steady level whether under effect of temperature ranging from 30 °C to 70 °C or pH (2, 4, 6 and 8), which proved that PO and IPO were insensitive to temperature and pH. A slight increase of PO and IPO was detected in the light of evaporation of water in the reaction system.

As illustrated in Fig. 2, exposed to β-glucosidase at 0.84 U/mL, PO was rapidly degraded into P in 6 h, the degradation rate of which was 96.8%. Nevertheless, IPO was found to be more obtuse, which decreased by 67% in 6 h and 94.1% within 18 h. There was a reciprocal transformation between (I)PO and (I)P, which suggested that β-glucosidase held an important role in

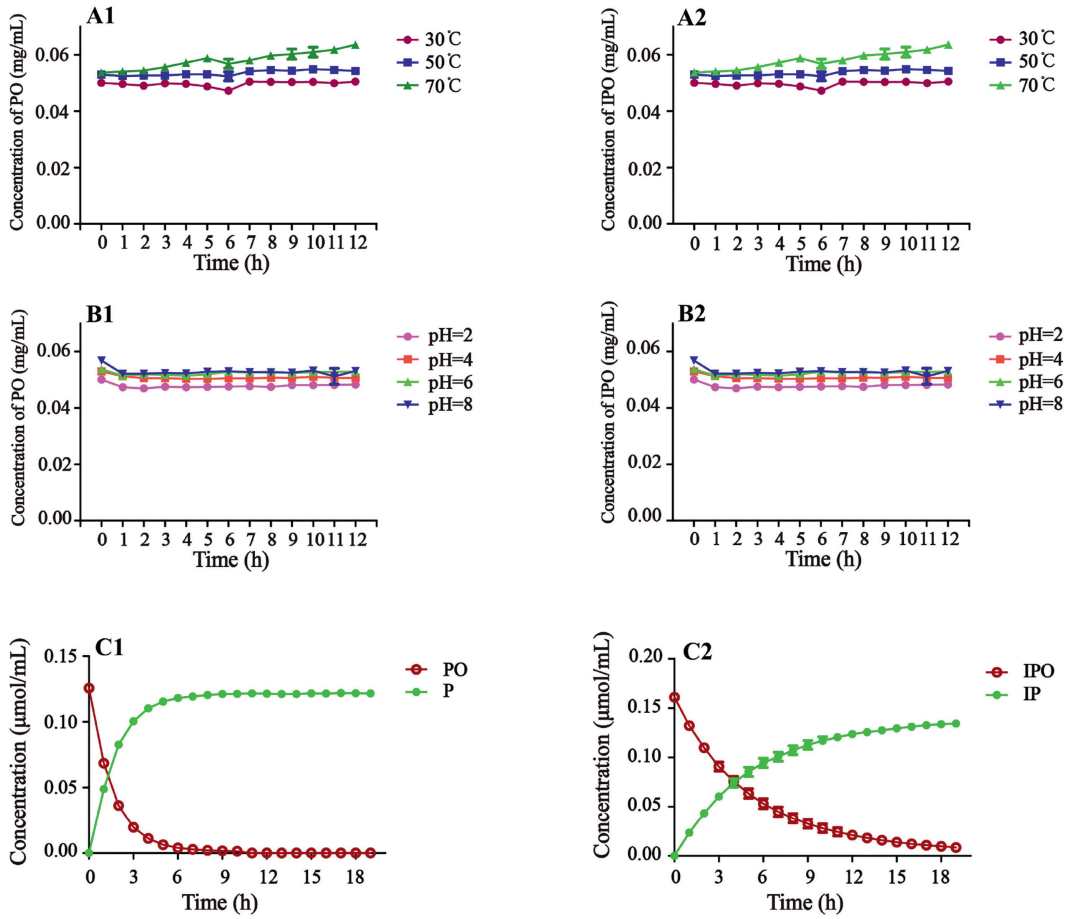

Fig. 2 – The dynamic variations of PO and IPO under different temperature (A1 and A2), pH (B1 and B2) and β-glucosidase at 0.84 U/mL (C1 and C2).

the conversion between (I)PO and (I)P and exerted an significant influence on the content of P and IP in FP.

3.3. Method validation

In view of the systematic study above, the method of ultrasonic extraction at 60 °C, which had high rate of extraction and efficiency, was validated methodologically including the linearity, LOD, LOQ, precision, repeatability, stability and accuracy of the interesting compounds, PO, IPO, P and IP. All calibration curves showed good linearity ($r \geq 0.9999$) across the test ranges and the overall LOD and LOQ values were less than 0.08 and 0.25 μg/mL, respectively. The RSDs of the intra- and inter-day precisions, repeatability, and stability were all below 3.0%. The average recoveries of the investigated targets were in the range of 98.30%–101.44% with RSD value below 2.98%. These results demonstrated that the established method was satisfactory for the simultaneous determination of PO, IPO, P and IP in FP.

3.4. Quantitative analysis of the samples from the different origins

The established method was applied in outlining the trends on content of the interesting targets of FP from ninety-six origins. Exhibited in Fig. 3A, the total content of P and IP from 0.011 to 0.120 mmol/g was distributed in a scattered form, however, the sum of PO, IPO, P and IP in the range of 0.111–0.170 mmol/g showed in narrow distribution. It could be speculated that the different activity of β-glucosidase contributed to the different degree of transformation between (I)PO and (I)P in the course of cultivation or processing, leading to the different level of P and IP from ninety-six origins.

Specifically, the distribution of total content of P and IP in FP from ninety-six origins was presented in detail in Fig. 3B. The total content of P and IP was divided into the following stages: 0.01–0.024 mmol/g which accounted for 25.00%, 0.024–0.038 mmol/g which made up 31.25%, 0.038–0.052 mmol/g in the proportion of 20.83%, 0.052–0.066 mmol/g which shared 11.46%, 0.066–0.08 mmol/g whose proportion was 8.33%, and 0.08–0.094 mmol/g, 0.094–0.108 mmol/g and 0.108–0.122 mmol/g only accounting for 3.12%, respectively. Released by ChP, the total content of P and IP must be no less than 0.70% (0.038 mmol/g) [1], which qualified only about 43.75% FP. From the performed study, an important clue can be conferred that the great attention should be paid to the effect of β-glucosidase on the content of P and IP. Many impact factors contributed to the activity of β-glucosidase should be profoundly mined to improve the quality of FP, including growth period, collecting season, processing procedure and storage time.

3.5. Chemical identification of the roasted from raw FP

Based on the fact that PO and IPO extracted from the raw and soaked FP can be rapidly and obviously transformed into P and IP in 50% methanol aqueous solution or less methanol in solution, which was not applicable to the roasted FP. But, transformation between (I)PO and (I)P was not detected in methanol extract of the raw, soaked or roasted FP. Making the best of this phenomenon originated from the effect of β-glucosidase, in order to prove the feasibility of identifying the roasted from raw and soaked FP, we employed methanol and 50% methanol aqueous solution as the extraction solution to extract the raw FP (B-5, B-51 and B-96), the dried FP under the shade after being soaked with 4% salt solution (SK-5, SK-51 and SK-96) and the salt-processed FP, i.e. the roasted FP after being soaked with 4% salt solution (SP-5, SP-51 and SP-96), respectively. The determined results and representative chromatograms of samples were shown in Table 1 and Fig. 4, respectively. As displayed in Table 1, the content of PO, IPO, P and IP in FP extracted by 50% methanol aqueous solution was tagged as C_{PO}, C_{IPO}, C_P and C_{IP}, whose content of PO, IPO, P and IP extracted by methanol was marked as C'_{PO}, C'_{IPO}, C'_P and C'_{IP}. The ratio of content of PO, IPO, P and IP in FP extracted by 50% methanol aqueous solution to that obtained by methanol was assigned as N_{PO}, N_{IPO}, N_P and N_{IP}, respectively, which was utilized to decide whether FP was roasted or not. Calculating formulae were as follows.

$$N_{PO} = C_{PO}/C'_{PO} \quad N_{IPO} = C_{IPO}/C'_{IPO}$$

$$N_P = C_P/C'_P \quad N_{IP} = C_{IP}/C'_{IP}$$

As illustrated from the result of the studied sample, the roasted FP (SP-5, SP-51 and SP-96) has given $0.9 \leq N_{PO}$ and $N_{IPO} \leq 1.1$ or N_P and $N_{IP} \leq 1.1$, and the unroasted FP (B-5, B-51 and B-96, and SK-5, SK-51 and SK-96) has shown N_{PO} and $N_{IPO} \leq 0.9$ or N_P and $N_{IP} \geq 1.1$. Therefore, according to the value of N_{PO}, N_{IPO}, N_P and N_{IP}, we can identify the roasted FP (the salt-processed FP) from unroasted FP (the raw FP and the dried FP under the shade after being soaked with 4% salt solution).

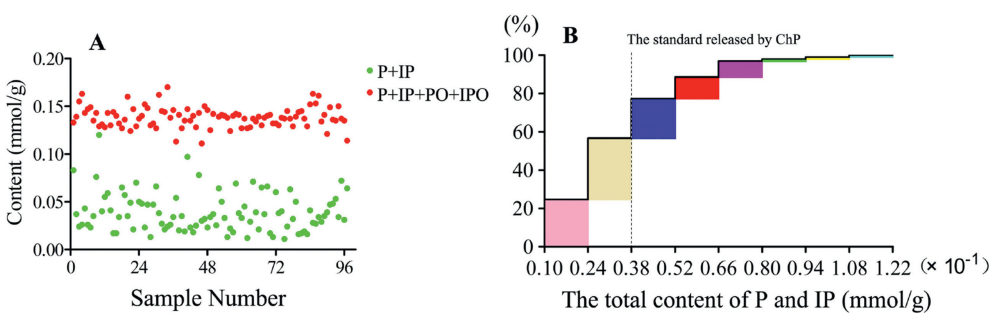

Fig. 3 – The scattering diagram (A) and accumulative histogram (B) of interesting compounds of FP from the different origins.

Table 1 – The contents of PO, IPO, P and IP in FP extracted by 50% methanol aqueous solution and methanol (mmol/g) and the value of N_{PO}, N_{IPO}, N_P and N_{IP}.

Sample	C_{PO}	C_{IPO}	C_P	C_{IP}	C'_{PO}	C'_{IPO}	C'_P	C'_{IP}	$^aN_{PO}$	$^aN_{IPO}$	^aN_P	$^aN_{IP}$
B-5	0.0194	0.0077	0.0485	0.0483	0.0524	0.0418	0.0207	0.0188	0.370	0.184	2.343	2.569
SK-5	0.0087	0.0034	0.0597	0.0530	0.0472	0.0379	0.0258	0.0225	0.184	0.090	2.314	2.356
SP-5	0.0464	0.0316	0.0226	0.0242	0.0478	0.0326	0.0246	0.0265	0.971	0.969	0.919	0.913
B-51	0.0147	0.0046	0.0523	0.0468	0.0563	0.0417	0.0156	0.0139	0.261	0.110	3.353	3.367
SK-51	0.0096	0.0039	0.0585	0.0492	0.0500	0.0374	0.0208	0.0179	0.192	0.104	2.813	2.749
SP-51	0.0511	0.0340	0.0185	0.0193	0.0525	0.0351	0.0199	0.0209	0.973	0.969	0.930	0.923
B-96	0.0139	0.0068	0.0524	0.0459	0.0326	0.0244	0.0352	0.0298	0.426	0.279	1.489	1.540
SK-96	0.0165	0.0085	0.0496	0.0437	0.0299	0.0229	0.0410	0.0334	0.552	0.371	1.210	1.308
SP-96	0.0291	0.0197	0.0387	0.0333	0.0289	0.0196	0.0398	0.0345	1.007	1.005	0.972	0.965

[a] $N_{PO} = C_{PO}/C'_{PO}$ $N_{IPO} = C_{IPO}/C'_{IPO}$ $N_P = C_P/C'_P$ $N_{IP} = C_{IP}/C'_{IP}$.

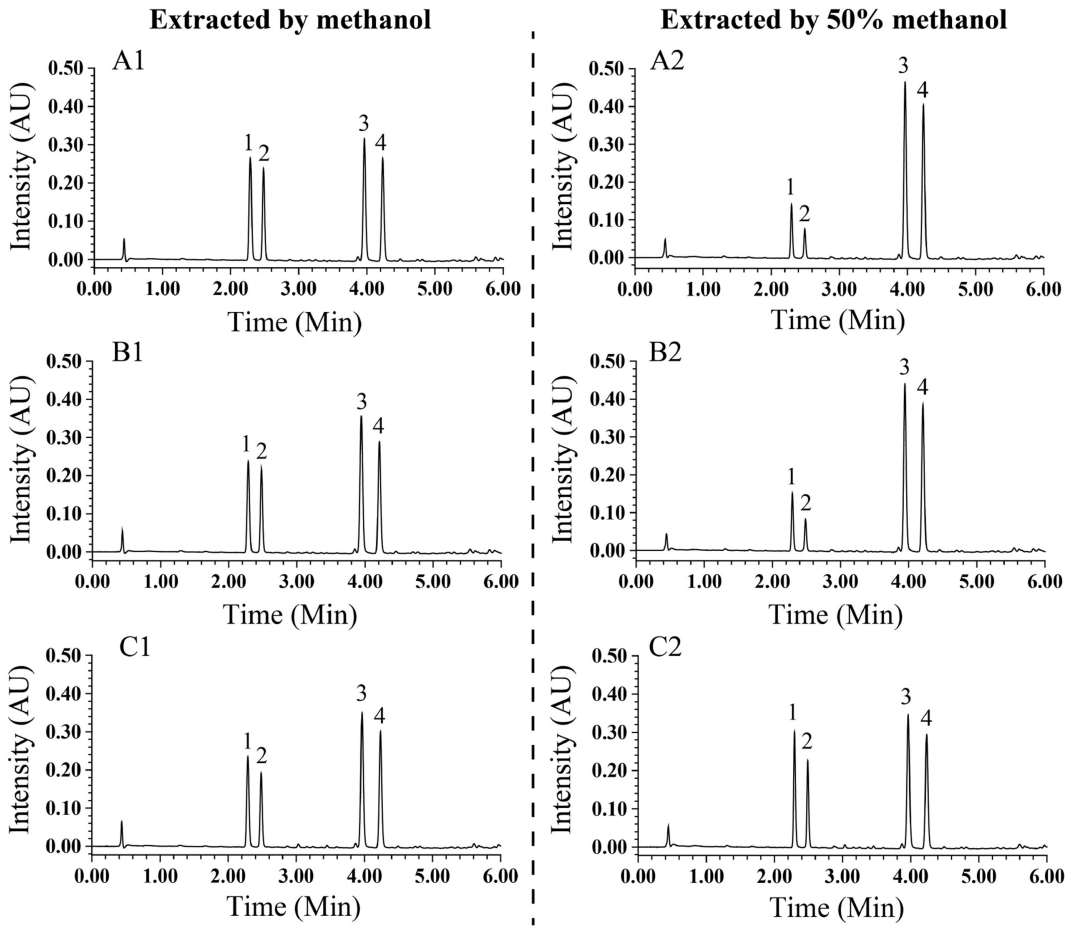

Fig. 4 – The representative chromatograms of samples B-5 (A1 and A2), SK-5 (B1 and B2) and SP-5 (C1 and C2) extracted by methanol and 50% methanol aqueous solution, respectively (1, PO; 2, IPO; 3, P; 4, IP).

4. Conclusion

In this study, a rapid and effective method based on UPLC has been developed for the quantification of PO, IPO, P and IP in FP, which was successfully applied in illustrating the important role of β-glucosidase in transformation between (I)PO and (I)P, surveying the quality of FP from the different origins, and identifying the roasted from unroasted FP. The result could pave the way for improving the quality and promoting the quality standard of FP.

Acknowledgments

This work was supported by the National Science and Technology Major Projects for "Major New Drugs Innovation and

Development" (grant number 2015ZX09J15102-004-004), the Tianjin Support Plans for the Top of the Notch Youth Talents, the National Natural Science Foundation of China (81403060) and National basic scientific and technological project (2014FY111100).

Appendix A. Supplementary data

Supplementary data related to this article can be found at https://doi.org/10.1016/j.jfda.2017.10.009.

REFERENCES

[1] National Commission of Chinese Pharmacopoeia. Pharmacopoeia of the People's Republic of China, vol. 1. Beijing: Chinese Medical Science and Technology Press; 2015. p. 188.
[2] Li X, Lee YJ, Kim YC, Jeong GS, Cui HZ, Kim HY, et al. Bakuchicin induces vascular relaxation via endothelium-dependent NO-cGMP signaling. Phytother Res 2011;25:1574–8.
[3] Li WD, Yan CP, Wu Y, Weng ZB, Yin FZ, Yang GM, et al. Osteoblasts proliferation and differentiation stimulating activities of the main components of Fructus Psoraleae Corylifoliae. Phytomedicine 2014;21:400–5.
[4] Yin S, Fan CQ, Wang Y, Dong L, Yue JM. Antibacterial prenylflavone derivatives from *Psoralea corylifolia*, and their structure-activity relationship study. Bioorg Med Chem 2004;12:4387–92.
[5] Zhang X, Feng J, Mu K, Ma H, Niu X, Liu C, et al. Effects of single herbal drugs on adhesion and migration of melanocytes. J Tradit Chin Med 2005;25:219–21.
[6] Shin HJ, Shon DH, Youn HS. Isobavachalcone suppresses expression of inducible nitric oxide synthase induced by Toll-like receptor agonists. Int Immunopharmacol 2013;15:38–41.
[7] Lee KM, Kim JM, Baik EJ, Ryu JH, Lee SH. Isobavachalcone attenuates lipopolysaccharide-induced ICAM-1 expression in brain endothelial cells through blockade of toll-like receptor 4 signaling pathways. Eur J Pharmacol 2015;754:11–8.
[8] Jung B, Jang EH, Hong D, Cho IH, Park MJ, Kim JH. Aqueous extract of *Psoralea corylifolia* L. inhibits lipopolysaccharide-induced endothelial–mesenchymal transition via downregulation of the NF-kappaB-SNAIL signaling pathway. Oncol Rep 2015;34:2040–6.
[9] Hsieh MJ, Chen MK, Yu YY, Sheu GT, Chiou HL. Psoralen reverses docetaxel-induced multidrug resistance in A549/D16 human lung cancer cells lines. Phytomedicine 2014;21:970–7.
[10] Liu X, Nam JW, Song YS, Viswanath AN, Pae AN, Kil YS, et al. Psoralidin, a coumestan analogue, as a novel potent estrogen receptor signaling molecule isolated from *Psoralea corylifolia*. Bioorg Med Chem Lett 2014;24:1403–6.
[11] Park J, Kim DH, Ahn HN, Song YS, Lee YJ, Ryu JH. Activation of estrogen receptor by bavachin from *Psoralea corylifolia*. Biomol Ther (Seoul) 2012;20:183–8.
[12] Seo E, Lee EK, Lee CS, Chun KH, Lee MY, Jun HS. *Psoralea corylifolia* L. seed extract ameliorates streptozotocin-induced diabetes in mice by inhibition of oxidative stress. Oxid Med Cell Longev 2014;2014:897296.
[13] Cheung WI, Tse ML, Ngan T, Lin J, Lee WK, Poon WT, et al. Liver injury associated with the use of Fructus Psoraleae (Bol-gol-zhee or Bu-gu-zhi) and its related proprietary medicine. Clin Toxicol (Phila) 2009;47:683–5.
[14] Wang X, Lou YJ, Wang MX, Shi YW, Xu HX, Kong LD. Furocoumarins affect hepatic cytochrome P450 and renal organic ion transporters in mice. Toxicol Lett 2012;209:67–77.
[15] Wang YF, Liu YN, Xiong W, Yan DM, Zhu Y, Gao XM, et al. A UPLC-MS/MS method for *in vivo* and *in vitro* pharmacokinetic studies of psoralenoside, isopsoralenoside, psoralen and isopsoralen from *Psoralea corylifolia* extract. J Ethnopharmacol 2014;151:609–17.
[16] Liu CX, Chen SL, Xiao XH, Zhang TJ, Hou WB, Liao ML. A new concept on quality marker of Chinese materia medica: quality control for Chinese medicinal products. Chinese Traditional and Herbal Drugs 2016;47:1443–57 [in Chinese, English abstract].
[17] Koyu H, Haznedaroglu MZ. Investigation of impact of storage conditions on *Hypericum perforatum* L. dried total extract. J Food Drug Anal 2015;23:545–51.
[18] Li XD, Cheng LP, Gu XZ, You XQ, Mao SJ. Study on quality standards of prepared slices of salt-processed *Psoralea corylifolia*. Chin J Inf TCM 2008;4:51–3 [in Chinese, English abstract].
[19] Qiao CF, Han QB, Song JZ, Mo SF, Kong LD, Kung HF, et al. Quality assessment of Fructus Psoraleae. Chem Pharm Bull (Tokyo) 2006;54:887–90.
[20] Cui Y, Taniguchi S, Kuroda T, Hatano T. Constituents of *Psoralea corylifolia* fruits and their effects on methicillin-resistant staphylococcus aureus. Molecules 2015;20:12500–11.
[21] Qiao CF, Han QB, Song JZ, Mo SF, Kong LD, Kung HF, et al. Chemical fingerprint and quantitative analysis of Fructus Psoraleae by high-performance liquid Chromatography. J Sep Sci 2007;30:813–8.
[22] Wang YF, Wu B, Yang J, Hu LM, Su YF, Gao XM. A rapid method for the analysis of ten compounds in *Psoralea corylifolia* L. by ultra performance liquid chromatography. Chromatographia 2009;70:199–204.
[23] Pandey A, Niranjan A, Misra P, Lehri A, Tewari SK, Trivedi PK. Simultaneous separation and quantification of targeted group of compounds in *Psoralea corylifolia* L. using HPLC-PDA-MS-MS. J Liq Chromatogr R T 2012;35:2567–83.
[24] Kar B, Verma P, Patel GK, Sharma AK. Molecular cloning, characterization and in silico analysis of a thermostable β-glucosidase enzyme from putranjiva roxburghii with a significant activity for cellobiose. Phytochemistry 2017;140:151–65.
[25] Mateos SE, Cervantes CA, Zenteno E, Slomianny MC, Alpuche J, Hernández-Cruz P, et al. Purification and partial characterization of β-glucosidase in chayote (Sechium edule). Molecules 2015;20:19372–92.
[26] Yang J, Jiang ZZ, Chai X, Zhao BC, Zhao XP, Wang YF. Discriminant analysis of "Q-Markers" of traditional Chinese medical injections – taking Dan Hong injection as a model. Modernization of Traditional Chinese Medicine and Materia Medica – World Science and Technology 2016;18:2056–61 [in Chinese, English abstract].
[27] Jiang ZZ, Wang YF. A pattern of hierarchical progression for quality standard of Chinese materia medica based on "herbal origin-material basis-quality markers-quality control method". Chinese Traditional and Herbal Drugs 2016;47:4127–33 [in Chinese, English abstract].

Available online at www.sciencedirect.com

ScienceDirect

journal homepage: www.jfda-online.com

Original Article

Nanoparticle based bio-bar code technology for trace analysis of aflatoxin B1 in Chinese herbs

Yu-yan Yu, Yuan-yuan Chen, Xuan Gao, Yuan-yuan Liu, Hong-yan Zhang, Tong-Ying Wang*

College of Pharmacy, Fujian University of Traditional Chinese Medicine, Fuzhou 350122, China

ARTICLE INFO

Article history:
Received 21 June 2017
Received in revised form
10 October 2017
Accepted 1 November 2017
Available online 6 December 2017

Keywords:
Aflatoxin B1
Bio-bar code assay
Chinese herbs
Magnetic microparticle probes
Nanoparticle probes

ABSTRACT

A novel and sensitive assay for aflatoxin B1 (AFB1) detection has been developed by using bio-bar code assay (BCA). The method that relies on polyclonal antibodies encoded with DNA modified gold nanoparticle (NP) and monoclonal antibodies modified magnetic microparticle (MMP), and subsequent detection of amplified target in the form of bio-bar code using a fluorescent quantitative polymerase chain reaction (FQ-PCR) detection method. First, NP probes encoded with DNA that was unique to AFB1, MMP probes with monoclonal antibodies that bind AFB1 specifically were prepared. Then, the MMP-AFB1-NP sandwich compounds were acquired, dehybridization of the oligonucleotides on the nanoparticle surface allows the determination of the presence of AFB1 by identifying the oligonucleotide sequence released from the NP through FQ-PCR detection. The bio-bar code techniques system for detecting AFB1 was established, and the sensitivity limit was about 10^{-8} ng/mL, comparable ELISA assays for detecting the same target, it showed that we can detect AFB1 at low attomolar levels with the bio-bar-code amplification approach. This is also the first demonstration of a bio-bar code type assay for the detection of AFB1 in Chinese herbs.

1. Introduction

Aflatoxins (AFs) which belong to a closely related group of secondary fungal metabolites, are toxic and highly carcinogenic substances [1,2]. AFs types include B1, B2, G1, or G2. The mould phenomenon occurred commonly in the cultivation, processing and storage period of medicinal materials, which may result in production of mycotoxins [3]. Mycotoxin contaminations caused by fungi are major issues related to the quality and safety of herbal medicine. AFs exposure remains an important aspect of herbal medicine safety which needs to be paid great attention. Failure to control such contamination may result in serious, even fatal, consequences for the consumers. Thus, some countries have set a limit for the amount of AFs that herbs may contain. In 2001, China promulgated the "Green Industry Standard for Import and Export of Medicinal Plants and Preparations" (WM2-2001), where AFs content limit was set as 5 μg/kg [4]. In 2008, the Food and Drug Administration of Korea issued a directive stipulating that

* *Corresponding author*.
E-mail address: yyyfj@163.com (Y.-y. Yu).

https://doi.org/10.1016/j.jfda.2017.11.003

Chinese herbs, including licorice, cassia, peach, Breit, Bozi, areca, Semen, Zhiyuan, and safflower, should have a maximum AFB1 amount of only 10 μg/kg [5]. In Italy a law sets guide-values AFB1 5 μg/kg and total AFs 10 μg/kg [6]. "Chinese Pharmacopoeia" 2015 version set the maximum limit of AFs in Cassiae, Polygalae radix, Platycladi semen, Peach, Ziziphi spinosae semen, etc, to 5 μg/kg [7]. As people are becoming more aware of the hazards of AFs and of the safety and quality of foods and drugs, the government has become stringent in regulating the AFs content, and thus called for the development of technology for the rapid detection of AFs. At present the mainly methods of detecting AFs are spectrometry, chromatography, immunoassay and biosensors [8–15]. However, these techniques produce limited sample throughput because of the time-consuming data extraction and cleansing.

The bio-bar code assay technology (BCA) was first introduced in 2003 by Mirkin, as a promising analytical tool for high sensitivity detection of proteins and nucleic acids [16]. The bio-bar code assay relies on a sandwich structure based on specific biological interaction of a magnetic particles and a nanoparticle with a defined biological molecule in a medium [17]. The magnetic particle allows the separation of reacted target molecules from unreacted ones. The nanoparticles aim at amplifying and detecting the target of interest. It uses magnetic microspheres to coat the target antiproteins; these beads have a diameter of up to a few microns [18]. BCA is a low-cost technology that exhibits high sensitivity for it uses gold nanoparticles for signal amplification. Each gold nanoparticle with a diameter of 30 nm can mark about 400 DNA barcode detection regions. Magnetic field causes the gold nanoparticles to form a complex with its target and magnetic microspheres. Subsequently, the DNA barcode chain is released from the gold nanoparticles, and these chains are detected through a variety of methods [19–23]. BCA exhibits the sensitivity of polymerase chain amplification technique, although it does not require enzymatic amplification reaction. The outstanding feature of this method is its high sensitivity, wherein it can detect antigenic concentrations as low as a few hundred molecules, the detection limit is lower than any existing methods [24,25]. Polymerase chain reaction was introduced in 1985 and has revolutionized biology and molecular biology since then. Its sensitivity allows the detection of 5–10 copies of DNA. However some drawbacks such as its complexity, time consuming procedure and narrow target have motivated the findings of new technologies. BCA technology is currently applied in the detection of nucleic acids and proteins; however, it is less applied in the detection of small molecules compounds [26–29].

This study established a highly sensitive novel technology for the rapid detection of AFB1. Similar to that of PCR, the sensitivity of BCA allows for the detection of biological molecules at a very low concentration. Thus, BCA may be used in the determination of AFB1, which exists in trace amounts in Chinese herbs. BCA may also be applied in the detection of other small molecule compounds. The linearity, accuracy, method precision, and system precision of BCA has already been validated. This is the first demonstration of a bar code type assay for the detection of AFB1.

2. Experimental

2.1. Materials and equipment

AFB1 polyclonal antibody and monoclonal antibody was prepared in ourselves lab. Chloroauric acid and sodium citrate from Sigma was used without further purification. Barcode DNA chain and complementary probe NP chain were purchased from Sangon Biotech (Shanghai). All reagents were prepared using analytical grade reagents and doubly distilled water. The gold nanoparticles were measured using transmission electron microscope (Hitachi High Tech International Trading Co. Ltd.). The magnetic microparticle MMP probes were measured using scan electron microscope (type JSM-7800F, JEOL Co.Ltd.). The barcode DNA chain was detected by fluorescence quantitative polymerase chain reactor (type H-7900, Biosystems Co., USA).

2.2. Preparation of gold nanoparticles

50 mL of boiling doubly distilled water was added to a 100 mL round bottom flask, and 0.5 mL 1% chloroauric acid solution was added quickly. With the high-speed stirring, 0.9 mL l% sodium citrate solution was added. Continue to boil until the solution turns red, and keep the red unchanged for 15 min. After cooling, the solution was constant volume in 50 mL volumetric flask, the products were stored in a dark place at 4 °C with 1% NaN_3. The gold nanoparticles were diluted to a certain concentration, and a small amount of them were put on the support film. The morphology of the gold nanoparticles was observed under transmission electron microscope (TEM).

2.3. Preparation of NP probe

A total of 10 mL of gold nanoparticles were collected, and their pH was adjusted to the optimum level use 0.1 mol/L K_2CO_3. About 1.3 mg of AFB1 polyclonal antibody was added, and stirring for 10 min. After 1 mL of 11% BSA was added dropwise, the mixture was left to stand for 30 min and then centrifuged at 4 °C. The precipitate was suspended to the original volume with 0.01 mol/L pH 7.6 PBS containing 1% BSA. After balancing overnight and centrifuging twice, the precipitate was suspended in 1 mL of PBS. A total of 1 mL of gold nanoparticles was decorated with AFB1 polyclonal antibody, and 500 μL of complementary probe NP chain with the concentration 2 μmol/L was added. The mixture was left to stand for 16 h at 25 °C, PBS solution was used to adjust the pH to 7.0, and ion concentration was increased use 0.1 mol/L NaCl. The solution was left to stand for 40 h at 25 °C. To obtain gold nanoparticles decorated with complementary probe NP chain after centrifugation for 30 min at 10 000 r/min, the precipitate was washed using 0.1 mol/L NaCl and 0.01 mol/L PBS (pH 7.0) three times, and then the unlabeled gold nanoparticles were deleted. A 500 μL solution of barcode DNA chain (concentration 2 μmol/L) was added to the above-mentioned gold nanoparticles decorated with complementary probe NP chain to hybridize for 4 h at 25 °C, and then centrifugation was performed for 30 min at 14 000 r/min to obtain the NP probe. The precipitate was then dissolved using 0.1 mol/L NaCl and 0.1 mol/L PBS (pH 7.0).

2.4. Preparation of MMP probe

The magnetic beads were lightly shaken for 5 min, and then 200 μL of these beads were collected to prepare a re-suspension with 2 mL of PBS, and 200 μL of PBS re-suspension magnetic beads was saved for later use. A total of 1.6 mL PBS was used to induce vigorous oscillation, and the supernatant was discarded by magnetic separation. The above steps were repeated four times. The solution was vigorously oscillated after adding 0.8 mL of 5% glutaraldehyde and then placed in a centrifugal tube in a nonmagnetic mixer to induce reaction for 3 h. The solution was vigorously oscillated again after adding 1.6 mL of PBS. The above steps were repeated four times after discarding the supernatant through magnetic separation.

A total of 60 μg of AFB1 monoclonal antibody was dissolved in 12 mL of PBS. The solution was vigorously oscillated after adding active magnetic beads and then placed in a mixer for mixing reaction of 20 h. The magnetic beads were re-suspended in 24 mL of PBS and vigorously oscillated after adding 12 mL of quenching agent (0.1 mol/L glycine). The solution was then placed in a mixer to enable reaction for 30 min. After washing three times with PBS, the supernatant was discarded through magnetic separation. Then, 1.6 mL of solution was used to resuspend the magnetic beads, and temperature was maintained at 4 °C.

2.5. Preparation of MMP-AFB1-NP sandwich structure

A total of 10 fg of AFB1 was added to 200 μL MMP probe with a vigorous oscillation at 37 °C for 1 h. Then fix MMP probe with a magnetic field and wash 4 times with PBS buffer solution in order to remove disconnected AFB1 antigen and other impure proteins. A total of 200 μL of gold nanoparticles decorated with double chain DNA and AFB1 polyclonal antibody were added, followed by vigorous oscillation for 30 min to form a sandwich structure. The MMP probe was fixed with magnetic field and washed four times with 400 μL of PBS buffer solution to remove disconnected NP probes.

2.6. Release of barcode DNA

A total of 100 μL of sterilized water was added to the sandwich structure, which was vigorously oscillated at 60 °C for 45 min to remove the hybrid from the barcode DNA chain. The MMP probe was then fixed with magnetic field, and the supernatant containing barcode DNA chain was collected. The bio-bar code assay allows for the amplification of the protein signal. Two binding events create a sandwich molecule. Bar-code DNA is released with the addition of water. The number of oligonucleotides released is proportional to the number of sandwich complexes formed. Here, the AFB1 isolated from the assay is detected, significantly amplifying the signal (Fig. 1).

2.7. FQ-PCR detection of barcode DNA chain

A Super Real Fluorescent quantitative premixed reagent detection kit (Tiangen Company) was used in this paper. The obtained barcode DNA chain was used as the template to enable FQ-PCR detection. FQ-PCR detection was performed using a two-step technique.

Primer 1: 5′-CGC ATT CAG GAT TGC ATG AT-3′
Primer 2: 5′-TAC GAC TTG ACA CCG TTA AG-3′
Barcode DNA chain: 5′-CGC ATT CAG GAT TGC ATG ATT GCC TCG TCT TAA CGG TCT CAA CTC GTA-3′
Complementary probe NP chain: 5′-TAC GAG TTG AGA CCG TTA AGA CGA GGC AAT CAT GCA ATC CTG AAT GCG A10-(CH2)6-SH-3′

2.8. Method validation

The method developed was validated for the detection of AFB1 in Chinese herb samples, including (Casslae semen, Polygalae

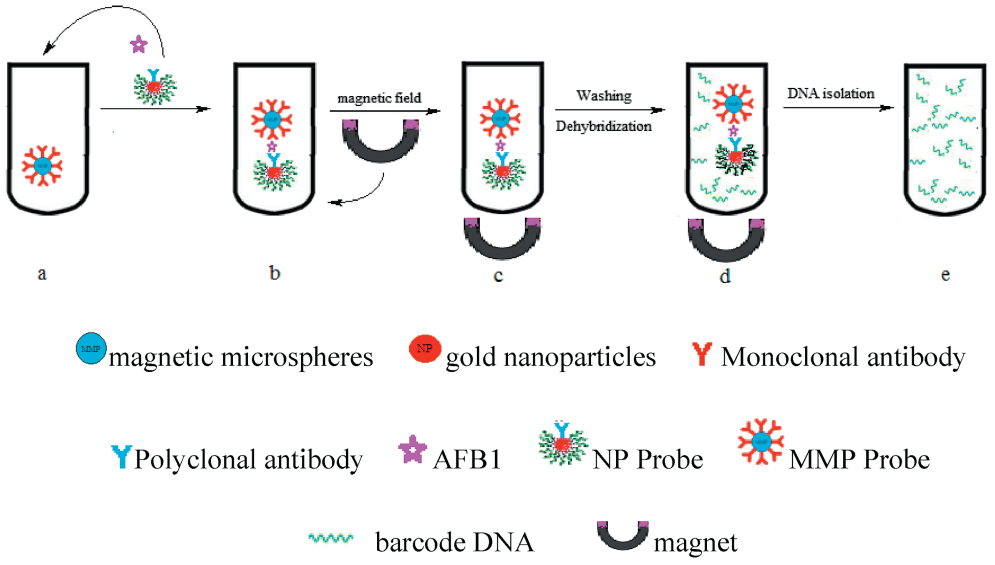

Fig. 1 – a: Interaction between MMP and target. b: Recognition between target and particles in complex biological medium: sandwich MMP-target-NP. c: Magnetic separation of MMP. d: Redispersion of sandwiches in distilled water causes dehybridization of bio-bar codes. e: Removal and analysis of bio-bar codes using FQ-PCR methods.

radix and Platycladi semen). Each sample was accurately weighed after drying into 10 mL centrifuge tubes and 2.5 mL of 75% methanol in water then added to extract AFB1 from the sample. After extraction, the solution was centrifuged 12 000 *g* for 12 min with Beckman Coulter XPN100 centrifuge (USA). The supernatant was filtrated and concentrated to 0.5 mL under a nitrogen steam. The residue was redissolved with 1 mL aqueous methanol solution and ready for FQ-PCR detection.

3. Results and discussion

3.1. *Identification of gold nanoparticles*

The colloidal gold was prepared by citrate sodium reduction method. The prepared gold nanoparticles were diluted to a certain concentration, and took a small amount added to the support film. After air drying, the gold nanoparticles, which were not muddy and had no sediment and flotsam, were observed under a transmission electron microscope. Observation through the transmission electron microscope revealed that the gold nanoparticles were round or oval with the same diameter, about 30 nm. UV–vis scanning was performed to prepare colloidal gold within the range of 200–800 nm. The highest absorption occurred at 520 nm. The results of TEM identification of gold nanoparticles, as shown in Fig. 2a, the morphology of gold nanoparticles are round or oval, the particle size is basically the same, the size is about 30 nm.

3.2. *Purification and identification of NP probe*

Excess electrolyte in the protein solution lowered the zeta potential of the colloid gold particles and affected protein absorption. Therefore, salt should be thoroughly removed before marking. Protein was dialyzed with low concentration saltwater (0.005 mol/L NaCl, pH 7.0) for 3 d, and the dialysate was changed every 6 h. The solution was then placed in a centrifuge at 12 000 r/min for 30 min at 4 °C, to remove the polymer. The unbalanced pH made the gold nanoparticles unstable. The optimal pH range was 7–8. To determine the optimal protein amount, >20% of the lowest stabilized amount obtained in the actual experiment was used because gold nanoparticles cannot be stabilized by an insufficient amount of AFB1 polyclonal antibody. Accordingly, 26 μg of polyclonal antibody was used in this experiment.

UV–vis scanning revealed that the λ_{max} of the NP probe was 528 nm. TEM revealed a gray black corona ring around the gold nanoparticles, showing that polyclonal protein was absorbed onto the particle surfaces (Fig. 2b). Previous studies have shown that the concentration of gold nanoparticles was about 0.106×10^{-11} mol/L.

3.3. *Preparation and determination of MMP probe*

Glutaraldehyde cross-linking method was used to activate the magnetic beads and examine the MMP probe using scan electron microscope (SEM). Before and after coupling reaction of the magnetic beads, the surface transformed from smooth to rough (Fig. 3). Magnetic bead coupling entirely proceeded

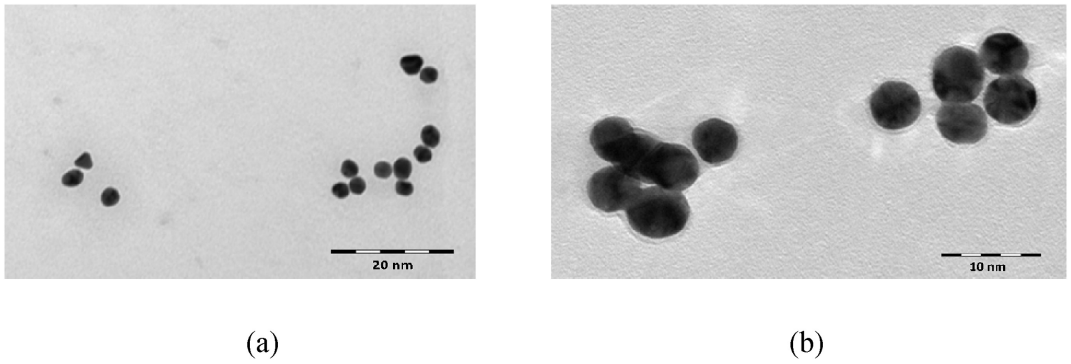

Fig. 2 – The TEM scan spectrum of gold nanoparticles (a) and NP probe (b).

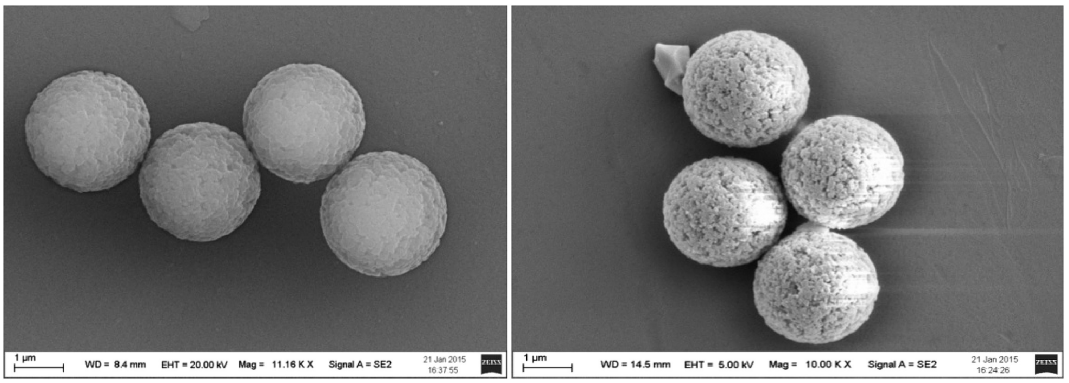

Fig. 3 – The SEM scan spectrum of magnetic beads and MMP probe. Note: Left—magnetic beads; Right—MMP probe.

in a mild environment. Changes in the surface indicated that coupling occurred between magnetic beads and AFB1 monoclonal antibodies. The entire process required a high magnetism for the beads. Therefore, washing was very critical to the process of activating and marking the beads, as well as to the formation of a sandwich structure and DNA release. Contaminated magnetic beads in any step can crucially affect the results. Only under high-temperature and low-salt conditions that double-chain DNA can be released. Therefore, the temperature should be controlled to obtain the DNA chain.

3.4. *Establishment of BCA detection system*

FQ-PCR amplification was conducted for the control sample diluted in a 10-fold gradient (10^{15}–10^{0} copies/μL). The standard amplification plot of FQ-PCR was showed on Fig. 4a. After the reaction was complete, the linear correlation between the Ct value and the copy number of the corresponding starting template was based to screen out five points (10^{15}–10^{11} copies/μL) within the linear range. At the same time, a better linear relationship was observed between them, and the standard curve was $y = -2.9054x + 54.581$ ($r = 0.9991$).

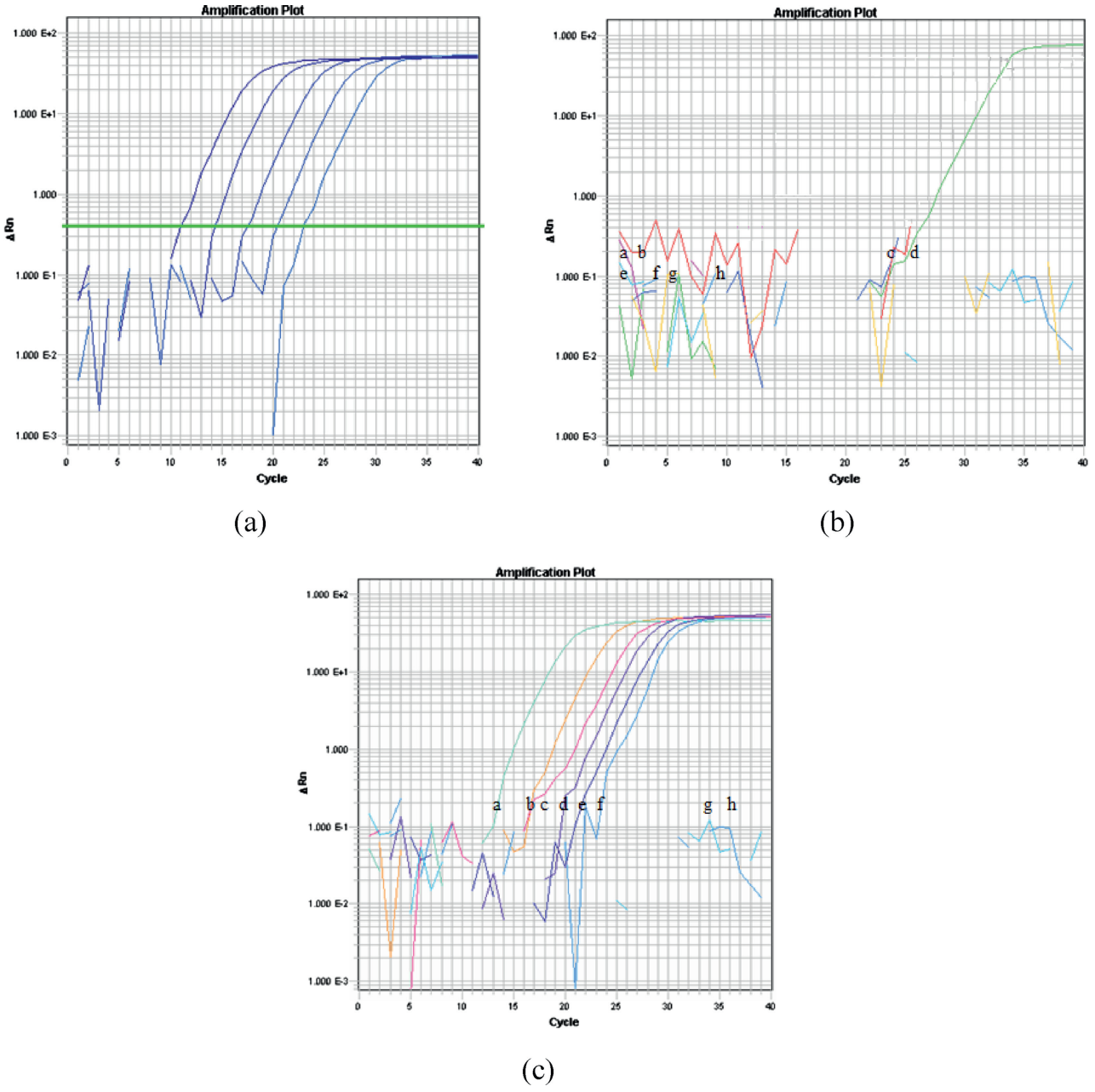

Fig. 4 – (a) The standard amplification plot of FQ-PCR. From left to right the copy numbers are 10^{15}, 10^{14}, 10^{13}, 10^{12} and 10^{11}. (b) The specificity test of FQ-PCR. a to h are AFB2, AFG1, AFG2, AFB1, Zearalenone, Vomitoxin, Fumonisins and Ochratoxin A respectively. (c) The sensitivity of FQ-PCR. The concentration of AFB1 are 10^{-3} ng/mL, 10^{-4} ng/mL, 10^{-5} ng/mL, 10^{-6} ng/mL, 10^{-7} ng/mL, 10^{-8} ng/mL, 10^{-9} ng/mL and 0 (a to h).

Table 1 – Determination of AFB1 spiked into Chinese herb samples.

Samples	Spiked concentration (ng/mL)	Mean recovery (%)	Intra-day repeatability[a]	Inter-day repeatability[b]
Casslae semen	2	94.3	3.26	3.28
	1	107.5	4.17	5.65
	0.2	93.2	5.84	7.26
Polygalae radix	2	92.5	2.90	3.45
	1	96.7	4.86	5.01
	0.2	104.5	4.34	6.52
Platycladi semen	2	90.6	2.69	4.33
	1	92.8	3.57	5.28
	0.2	95.1	5.38	8.63

[a] Intra-day repeatability was estimated by analysis of six replicate samples at two concentration level on the same day.
[b] Intra-day repeatability was estimated by analysis of six replicate samples at two concentration level in three day.

Table 2 – Comparison of the available methods for the detection of AFB1.

Method	Detection limit (ng/mL)	Sample Mean[a] ± SD[b] (ng/mL)			Reference
		Cassiae	Polygalae radix	Platycladi semen	
FQ-BCA	10^{-8}	0.302 ± 0.024	0.240 ± 0.017	0.151 ± 0.004	This work
HPLC	0.12	0.355 ± 0.047	0.297 ± 0.081	0.204 ± 0.053	[c]
ELISA	1.98	Not detected	Not detected	Not detected	[d]

[a] The mean of three experiments.
[b] SD = standard deviation.
[c] The results were obtained by HPLC using Pharmacopoeia of China method with modifications.
[d] The results were obtained using ELISA method with Wang TY, 2017.

3.4.1. *Repeatability*

To evaluate the practical applicability and accuracy of this method, it was validated for detection of AFB1 in Chinese herbs samples, which were spiked with AFB1 at 2 ng/mL, 1 ng/mL and 0.2 ng/mL concentrations levels. There recoveries were in the range of 90.6–107.5%. To calculate intra-assay and inter-assay repeatability, all measurements were done in triplicate. FQ-BCA detection results for different copy numbers showed that both of intra-assay and inter-assay CV values were <10%. The RSDs of the intra-day were in the range of 2.69–5.84%. Inter-day precision for each compound was also investigated with RSDs in the range of 3.45–8.63%. All these data revealed that the established method had an acceptable precision (Table 1).

3.4.2. *Specificity*

Seven mycotoxins were selected as interferences to determine the specificity of this method. 1 μg/mL of other six mycotoxins including zearalenone, vomitoxin, ochratoxin A, AFB2, AFG1, and AFG2 and 0.1 μg/mL AFB1 were examined respectively. Depends on the specificity of the monoclonal and polyclonal antibodies, AFB1 had no cross-reaction with zearalenone, vomitoxin, or ochratoxin A, AFB2, AFG1, and AFG2. The results indicated that the probes would not interact with other mycotoxins besides AFB1 (Fig. 4b).

3.4.3. *Sensitivity*

Following extensive experimentation with the FQ-PCR detection method, we were able to detect AFB1concentrations down to 10^{-8} ng/mL using the bio-bar code assay (Fig. 4c). FQ-PCR detection was performed for the barcode DNA chain obtained from release. This technique had high sensitivity for polymerase chain reaction, did not require enzyme amplification, and was able to detect antigenic substances with a wide concentration range, which have not been achieved by any existing quantitative immunoassay.

3.5. *Sample determination*

This method can be used for the trace determination of AFB1 in medicinal materials. FQ-PCR detection was performed for DNA released from the preparation of sandwich by using Chinese herb samples. As shown in Table 1, Casslae semen, Polygalae radix, Platycladi semen had cycles of 21.23, 21.62, and 21.11, respectively. Using the standard curve, the obtained copy numbers were $10^{11.48}$, $10^{11.38}$, and $10^{11.18}$, respectively, equal to AFB1 containing 0.302 ng/mL, 0.240 ng/mL, and 0.151 ng/mL. Accurate dropping of each reagent was very important; any tiny error can cause a large deviation through PCR magnification. To the best of our knowledge, this assay presents no serious hazards, though caution should be taken to avoid skin and eye contact with the AFB1 solution. In addition, when the assays are used in conjunction with unknown biological samples or known AFs samples, all proper government safety protocols should be followed. A highly sensitive method for detecting AFB1 through a nonenzymatic nanomaterials-based amplification method, the bio barcode assay is established. Compared with the currently available

instrumental and rapid screening methods, this method is more sensitive than ELISA [14,28] and HPLC [29] (Table 2). The experimental results demonstrate that the bio-bar code method can be used for rapid AFB1 detection.

4. Conclusions

A rapid and sensitive bio-bar code method for determination of AFB1 in Chinese herbs was well developed and validated, with the LOD at 10^{-8} ng/mL. This new method has been successfully applied to three different Chinese herbs. It is comparable to many PCR-based approaches without the need for enzymatic amplification. Because this method approach is a pseudohomogeneous system with both MMP and NP in solution, the probes can be used to very efficiently bind target, thereby reducing the time required for high sensitivity detection experiments. The results have laid important foundation for further improvement of detection standards for AFs in Chinese herbs and provided a new vision for the trace determination of other small molecular compounds. Indeed, an advantage of the method approach over conventional microarray sandwich assays is that the entire assay can be carried out in 3–4 h, regardless of target concentration. In consequence, the suggested technique could be a powerful method for AFB1 detection in the future.

Acknowledgment

This project was supported by the National Natural Science Foundation of China (No. 81202914), Guide the Project of Science and Technology Department of Fujian Province (No. 2016Y0056), and Key Projects of Fujian Province Health and Family Planning Commission (2015-ZQN-JC-33).

REFERENCES

[1] Peraica M, Radić B, Lucić A, Pavlović M. Toxic effects of mycotoxins in humans. Bull World Health Organ 1999;77:754–66.
[2] Hussein HS, Brasel JM. Toxicity, metabolism, and impact of mycotoxins on humans and animals. Toxicology 2001;167:101–34.
[3] Cai F, Gao WW, Li HL, Chen J, Li ZZ. Aflatoxin contamination of Chinese herbal medicine in China and its potential management strategies. Chin J Chin Mater Med 2010;35:2503–7.
[4] Li JY, Wan L, Yang MH. Limit standard of mycotoxins and advances in studies on its application in Chinese material medica. Chin Trad Herb Drugs 2011;42:602–9.
[5] Romagnoli B, Menna V, Gruppioni N, Bergramini C. Aflatoxins in spices, aromatic, herbs, herb-teas and medicinal plants marketed in Italy. Food Control 2007;18:697–701.
[6] Trucksess MW, Dombrink-kurtzman MA, Tournas VH, White KD. Occurrence of aflatoxins and fumonisins in Incaparina from Guatemala. Food Addit Contam 2002;19:671–5.
[7] Chinese Pharmacopoeia Commission. Pharmacopoeia of the People's Republic of China, 1 vols.. Beijing: China Medical Science Press; 2015. 145, 156, 247, 278, 375.
[8] Biancardi A, Dall'Asta C. A simple and reliable liquid chromatography-tandem mass spectrometry method for the determination of aflatoxin B_1 in feed. Food Addit Contam 2014;31:1736–43.
[9] Guo X, Wen F, Zheng N, Luo Q, Wang H, Li S, et al. Development of an ultrasensitive aptasensor for the detection of aflatoxin B1. Biosens Bioelectron 2014;56:340–4.
[10] Sheng YJ, Eremin S, Mi TJ, Zhang SX, Shen JZ, Wang ZH. The development of a fluorescence polarization immunoassay for aflatoxin detection. Biomed Environ Sci 2014;27:126–9.
[11] Sengul Umit. Comparing determination methods of detection and quantification limits for aflatoxin analysis in hazelnut. J Food Drug Anal 2016;24(1):56–62.
[12] Hickert S, Gerding J, Ncube E, Hübner F, Flett B, Cramer B, et al. A new approach using micro HPLC-MS/MS for multi-mycotoxin analysis in maize samples. Mycotoxin Res 2015;31:109–15.
[13] Tang D, Zhong Z, Niessner R, Knopp D. Multifunctional magnetic bead-based electrochemical immunoassay for the detection of aflatoxin B1 in food. Analyst 2009;134:1554–60.
[14] Yang L, Ding H, Gu Z, Zhao J, Chen H, Tian F, et al. Selection of single chain fragment variables with direct coating of aflatoxin B1 to enzyme-linked immunosorbent assay plates. J Agric Food Chem 2009;57:8927–32.
[15] Yang MH, Chen JM, Zhang XH. Immunoaffinity column clean-up and liquid chromatography with post-column derivatization for analysis of aflatoxins in traditional Chinese medicine. Chromatographia 2005;62:499–504.
[16] Nam J, Taxton CS, Mirkin CA. Nanoparticle-based Bio-barcodes for the ultrasensitive detection of proteins. Science 2003;301:1884–6.
[17] Stoeva SI, Lee JS, Thaxton CS, Mirkin CA. Multiplexed DNA detection with bio bar coded Nanoparticle probes. Angew Chem Int Ed Engl 2006;45:3303–6.
[18] Bao YP, Wei TF, Lefebvre PA, An H, He LX, Kunkel GT, et al. Detection of protein analytes via nanoparticle-based bio bar code technology. Anal Chem 2006;78:2055–9.
[19] Haley HD, Vega RA, Mirkin CA. Nonenzymatic detection of bacterial genomic DNA using the bio bar code assay. Anal Chem 2007;79:9218–23.
[20] Bi S, Zhou H, Zhang S. Bio-bar-code functionalized magnetic nanoparticle label for ultrasensitive flow injection chemiluminescence detection of DNA hybridization. Chem Commun (Camb) 2009;37:5567–9.
[21] Li XM, Wang LL, Luo J, Wei QL. A dual-amplified electrochemical detection of mRNA based on duplex-specific nuclease and bio-bar-code conjugates. Biosens Bioelectron 2015;15(65):245–50.
[22] Dong H, Meng X, Dai W, Cao Y, Lu H, Zhou S, et al. Highly sensitive and selective microRNA detection based on DNA-bio-bar-code and enzyme-assisted strand cycle exponential signal amplification. Anal Chem 2015;87(8):4334–40.
[23] Nie LB, Wang XL, Li S, Chen H. Amplification of fluorescence detection of DNA based on magnetic separation. Anal Sci 2009;25:1327–31.
[24] Nam JM, Stoeva SI, Mirkin CA. Bio-bar-code-based DNA detection with PCR-like sensitivity. J Am Chem Soc 2004;126:5932–3.
[25] An JH, Oh BK, Choi JW. Detection of dopamine in dopaminergic cell using nanoparticles-based barcode DNA analysis. J Biomed Nanotechnol 2013;9(4):639–43.

[26] Zhao LF, Li YY, Xu SQ. Nanoparticle based bio barcode method for trace analysis of dioxin like chemicals. Chin J Biochem Mol Biol 2009;25:188–92.
[27] Xu H, Zhu X, Ye H, Yu L, Chen G, Chi Y, et al. A bio-inspired sensor coupled with a bio-bar code and hybridization chain reaction for Hg^{2+} assay. Chem Commun (Camb) 2015;51:15031–4.
[28] Wang TY, Chen YY, Gao X, Yu YY. Study on rapid immunological detection method for determining AFB1 in traditional Chinese medicines. J Mod Med Health 2017;2(33):177–9.
[29] Chinese Pharmacopoeia Commission. Pharmacopoeia of the People's Republic of China, 4 vols.. Beijing: China Medical Science Press; 2015. p. 224.